

A MSC/DYTRAN SIMULATION OF THE LYNX HELICOPTER MAIN LIFTFRAME COLLAPSE

Marcio J. Cavalcanti

Brazilian Navy
Diretoria de Aeronautica da Marinha
Rio de Janeiro, RJ, Brazil

Rade Vignjevic

College of Aeronautics
Cranfield University
Cranfield, Bedford, United Kingdom

Abstract

MSC/DYTRAN, an explicit nonlinear finite element code, was used to determine the collapse characteristics of the Lynx helicopter main liftframe, for the vertical crash case. The liftframe was modelled by the Belytschko-Tsay four node shell elements. The analysis of the influence of the collapse velocity on the component structural failure modes and a sensitivity analysis of the material failure criteria were performed. The increase in crashing velocity from 4 to 8 m/s changed the mode of structural failure from torsional buckling, to bending/axial failure. The material failure criteria, however, did not significantly affect the structure collapse mechanism nor the force vs displacement results. The MSC/DYTRAN simulation results showed good agreement with the full scale test data.

1. Introduction

The main aim of a helicopter crashworthy design is to prevent occupant fatalities and to minimize the number and severity of injuries during specified crash events, while minimizing, to the maximum possible extent, aircraft damage. To achieve these goals, the dynamic forces experienced by the occupants should be reduced to acceptable levels, a survivable space envelope should be preserved and post-crash hazards eliminated. In addition, the occupants should be allowed to evacuate from the vehicle.

The Military Standard MIL-STD 1290A [1] is the document which entails the most comprehensive set of the crashworthiness requirements for light fixed and rotary-wing aircraft. It states that instrumented full scale tests are desirable but not mandatory if designer can demonstrate that, for each required impact condition, the deceleration of the structure, its trajectory and the occupant motion are compatible with the crashworthy design objectives.

Current techniques for structural crashworthiness evaluation are equally applicable to both automotive and aeronautical fields, and are classified [2-5] as:

- a) experimental - entails crash tests of real full scale vehicles, structural components or their scaled models;
- b) hybrid - is a combined experimental and numerical approach in which the structure is divided into a number of relatively large sections or subassemblies which are tested or analysed separately and their crash properties used in a simplified beam/non linear spring model of the whole structure.
- c) analytical - is based on the first principle finite element method which can deal with the material, geometrical and contact nonlinearities.

It is obvious that, the experimental technique is most reliable, but at the same time, it is usually unacceptably expensive because each test reflects only one point of the crash envelope.

On the other hand, the analytical approach has become a useful tool within the design process, but until very recently the computational problem associated with it was formidable and the computational costs and time necessary to perform it were extremely high.

Not surprisingly, the hybrid approach, a compromise between the two others techniques, has been the most commonly used method. Using simpler physical tests and numerical codes, like the program KRASH [6], designers have been taking advantage of the best in both other methods.

Instead of establishing crush characteristics of structural components by testing one can very effectively use analytical techniques. The ultimate purpose of this work is:

- to determine numerically the quasistatic collapse characteristics of a given helicopter liftframe corresponding to the vertical crash case needed for the hybrid analysis,
- to build a detailed component model which can be used as a part of the finite element model of the whole helicopter,
- to check MSC/DYTRAN effectiveness in this type of analysis.

2 The Lynx Helicopter Liftframe

Lynx is a medium sized helicopter with the maximum take-off gross weight of approximately 4500 kg designed by Westland in the late 60s, to fulfill general purpose, naval and civil transport roles. Although its semi-monocoque airframe had been designed to withstand the demanding landing conditions imposed by the ship flightdeck motion no detailed crashworthiness consideration has been done throughout the design process.

The Lynx rear fuselage structure and the main liftframe are shown in Figures 1 and 2, respectively. Those structures are manufactured in conventional aluminum alloy. The main gear box, the main rotor head and the rotor blades weighting approximately 870 kg represent the main source of the dynamic loads for the liftframe in the vertical crash case. This mass is attached to the main gear box support beams (item 1 in Figure 1). The front ends of the support beams are bolted to the main liftframe, and the rear ends are bolted to the bulkhead (respectively items 2 and 3 in Figure 1). These three components are the main load path for the dynamic loads and at the same time one of the main energy absorbing components in the vertical crash case.

3. Modelling the Liftframe

3.1 The Liftframe Geometry

The liftframe has one plane of symmetry (see Figure 2) and the vertical crash case is symmetrical with respect to the same plane so it was sufficient to analyse only one half of the liftframe. Thus the port side of the liftframe was analysed. The port side liftframe model is shown in Figure 3. It was built using four node one point quadrature Belytschko-Tsai shell elements. The mesh was positioned on the corresponding midplanes of the real liftframe. This element type was chosen for its accuracy, speed and reliability in large deformation nonlinear problems.

The one-point Gauss quadrature integration is largely used in order to reduce the number of operations executed during each integration time step. It is well known that this may give rise to spurious zero energy deformation modes (hourglass modes). In MSC/DYTRAN those modes can be stabilised by using an hourglass viscosity or an hourglass stiffness.

The underfloor part of the liftframe was not considered in this work because it is fully restrained by the rest of the helicopter underfloor structure so that it does not significantly influence the behaviour of the upper part of the liftframe.

A first model with a relatively coarse mesh was used to identify the liftframe overall mode of failure and the location of plastic hinges. Accordingly, the areas undergoing large deformations were further refined to improve the accuracy of the analysis without wasting extra computational time on an unnecessary general model refinement. The final mesh comprises 2613 shell elements, 2723 nodes and approximately 13000 degrees of freedom. Considering the average density of aluminum alloys, the model had a weight of 5.3 kg.

To incorporate the geometry imperfections generated by the component manufacturing process the nodes of the ideal (perfectly flat) mesh were randomly moved out of their original planes. These perturbations had a uniform distribution in the ± 0.15 mm interval, i.e. 8% of the smallest liftframe web thickness.

3.2 Boundary Conditions

The boundary conditions imposed to the liftframe model during the numerical simulation should be as close as possible to those experienced by the real component, under the same circumstances. Thus, boundary condition consideration was focused on the connections of the liftframe with the rest of the fuselage structure. The port side half of the liftframe is connected to the following components (see Figures 1 and 2):

- the starboard side half of the liftframe, at section A-A, by means of a strap joint;
- the aircraft skin, along the external flange, by means of rivets;
- the main gear box support beam, at point B, by bolts;
- the floor structure, in region C, by means of rivets and bolts.

The symmetry boundary conditions were applied to the nodes laying in the plane of symmetry.

It was assumed that the skin would impose some but not significant restraint to the liftframe external flange motion in the aircraft longitudinal and lateral directions. However, as deformations increase, rivets would probably fail, reducing these restrictions. Therefore, the skin influence on the liftframe collapse was ignored.

The very stiff main gearbox support beams constrain motion of the liftframe in the aircraft longitudinal direction. So it was assumed that the nodes corresponding to the support beam attachments do not move in the aircraft longitudinal direction as the liftframe collapses.

Due to the high stiffness of the underfloor structure, to which the liftframe is connected, it was assumed that the liftframe model was built into a rigid wall, i.e. the nodes laying in the floor plane were fully restrained.

3.3 Loads and Initial Conditions

The geometrical and structural aspects discussed above indicated that a purely vertical load applied on the nodes corresponding to the main gear box support beam attachments would be representative of the vertical impact case selected for analysis. For the purpose of determining the quasistatic collapse properties of the frame, a decision was made to impose a constant vertical velocity on the load bearing nodes.

The magnitude of the constant velocity load was chosen so that it is representative of the crash velocity, but at the same time it reduces the computing time. Considering that the time spent computing one integration time step did not depend of the crushing velocity, it is clear that for a same level of component deformation the total processing time was inversely proportional to the crushing velocity magnitude. An initial decision was made to use the same velocity indicated in the MIL-STD 1290(A) for the vertical impact with retracted landing gear, which is 8m/s[‡]. To assess any possible influence of the crushing velocity on the component behaviour, another analysis was performed loading the model at 4m/s.

As initial conditions, all nodes were assigned the same initial velocity of 4 and 8 m/s, for the two load cases, respectively.

3.4 The Material Model

The liftframe is made of a forged L77 aluminum alloy. A bilinear elastoplastic material with isotropic hardening model was used. The material properties were taken from the Military Handbook MIL-HDBK-5(F) [9]. Since aluminum alloys are not sensitive to strain rates up to 10^3 s^{-1} [10], no attempt was made to simulate any strain rate effect.

The adopted criteria for material failure was 12% [10, 11] of maximum equivalent plastic strain. Actually, the maximum equivalent plastic strain is the standard material failure criteria provided by MSC/DYTRAN. When an element fails, it is automatically deleted from the mesh.

Nevertheless, Stronge [12] comments that some aluminum alloys can experience strains as high as 18% before failing, while Duffey [13] has shown that the principal shear stresses seems to govern material separation, for some structures under impulse loading, and hence the Tresca criteria leads to more accurate results.

This motivated a sensitivity analysis entailing the effect of different material failure criteria on the numerical results. The following criteria were analysed:

- maximum equivalent plastic strain of 12%,
- maximum equivalent plastic strain of 18%,
- maximum shear stress, i.e. Tresca criteria.

[‡] Actually 7.9 m/s, but the difference is not significant in terms of results and makes the association between time and displacements more evident.

In the case of the maximum equivalent plastic strain, it was necessary just to change this parameter in the model bulk data. In the case of Tresca criteria, it was necessary to write a user defined FORTRAN subroutine. This subroutine calculated the principal stresses acting in each layer[§] of the shell elements, then calculated the mean value of the maximum shear stresses for the layers considered and compared it with the shear stress corresponding to the uniaxial tensile test ultimate shear stress. To avoid severe deterioration of the program performance, only the elements that could possibly fail were checked against the criterion.

4. The Liftframe Collapse Characteristics

A crashworthiness analysis entails the assessment of the following structural collapsing characteristics:

- the force vs displacement curves;
- the maximum crush loads;
- the energy absorbed by the structure;
- the collapse mechanism;
- the post-failure behaviour.

The force vs displacement curves and the maximum crush load determine the dynamic forces transmitted to other components and, when applicable, to the vehicle occupants. The structure energy absorption capacity defines the amount of the impact kinetic energy that the structure is capable of absorbing. The collapse mechanism and the post-failure behaviour establish whether the structure crash behaviour is compatible with the requirements of preserving a survivable envelope and an adequate evacuation path while preventing post-crash hazards for the aircraft occupants.

For the considered crash case, the displacements were measured at the points where the loads were applied. The external vertical force was computed by adding up the internal forces calculated by MSC/DYTRAN at the nodes of the model base (see Figure 2, cross section D-D).

5. Numerical Results

5.1 The Influence of Crushing Velocity

To assess any possible influence of the crushing velocity on the component behaviour, two analyses were performed crushing the model at 8m/s and at 4m/s. In both crash cases the structure behaviour was typical of axially loaded columns. The force vs displacement and the energy vs displacement curves obtained for these two cases are shown respectively in Figures 4 and 5. The curve segments between points A and B correspond to the structure linear-elastic behaviour, when it offers high resistance to the applied load. Between B and C the structure buckles, plastic hinges are formed, producing a mechanism inside the structure, and the component collapses with considerable reduction in its load carrying capacity. After C, a relatively small load

[§] Three integration points were used through the thickness of each shell.

characterises the post collapse behaviour of the structure. Accordingly the strain energy absorbed by the structure increases rapidly from A to C. The energy absorption rate considerably reduces after plastic hinges are formed.

The oscillations observed in the first 4mm of the force vs displacement curves are due to stress wave propagation and reflection inside the structure. Though these effects are irrelevant for these impact velocities, this result indicates the suitability of MSC/DYTRAN for stress waves propagation analysis.

Though the force vs displacement and the energy vs displacement curves are similar for both crash cases, the structural modes of failure are different. The liftframe buckles in torsion in the 4m/s crash, as can be seen in Figure 6. This figure presents the model deformed shape after 15ms of load application, which corresponds to 60 mm of displacement. In the 8m/s crash case, the structural mode of failure is different, being characterized by buckling of its lower panel, as Figure 7 shows. This figure presents the model deformed shape after 5 ms of load application, which corresponds to 40 mm of displacement. Most of the relevant plastic deformation is concentrated in this region.

The model deformed shapes for both 4m/s and 8m/s crashes were not shown at the same displacement value for clarity reasons. The torsional buckling mode is much more developed at 60mm than at 40mm. In the 8m/s crash case one can better observe the component mode of failure at 40mm of displacement, because at 60mm many elements of the mesh failed and the liftframe started unloading.

The difference of the structural modes of failure at these two crushing velocities accounts for the amplitude differences observed in the force vs displacement and in the energy vs displacement curves. In the 8m/s crash, inertial effects stabilize the structure, that collapses under higher loads and absorbs more strain energy than it does in the other crash case, up to the point when the plastic hinges form. In other words, at 8m/s the structure collapses at a higher energy mode.

After collapse, however, (point C in the energy vs displacement curves in Figure 5) the 4m/s crash absorbed energy at a higher rate than the other one, showing that its residual strength was also higher. This is consistent with the force results. It can be seen that the structure crashed at 4m/s retained higher load carrying capacity than the structure crashed at 8m/s, after plastic hinge formation.

It can also be observed that, at the vicinity of point D, the strain energy curve for the 8m/s crash shows severe singularities. Those singularities coincide with the moment when the liftframe splits into two pieces, since a whole chain of elements across the model width failed. No singularities are observed in the energy vs displacement curve of the 4m/s crash, which means that, in this case, the liftframe did not split into two pieces. Actually, after 80 mm of displacement, **not a single element failed** in the entire mesh. This must be attributed to the more uniform distribution of plastic deformation associated with the torsional buckling mode.

The analysis of the 8m/s crash took approximately 6 hours of CPU time on the CRAY J916 computer at Cranfield University. This analysis was terminated after 15 milliseconds of real time (120 mm of displacement), with a total of 49500 time steps (2.3 steps/sec). The contact calculation used 16% of CPU time. The calculated speed of sound in the modelled material was 5.44×10^3 m/s and the stable time step 3.07×10^{-7} seconds.

4.3 The Effect of Failure Criteria

A sensitivity analysis entailing the effect of different material failure criteria on the numerical results was performed, and the following criteria were analysed:

- maximum equivalent plastic strain of 12%,
- maximum equivalent plastic strain of 18%,
- maximum shear stress, i.e. Tresca criteria.

For the three cases the liftframe mode of failure was the same, characterized by buckling of the lower panel. This is illustrated in Figure 8 which shows three different pictures of the model crushed at 8m/s after 5.0 ms of load application (i.e. 40mm displacement). The first picture, corresponds to the analysis where the 12% maximum equivalent plastic strain criteria was applied. The second picture shows the model deformation when the failure criteria was changed to 18% maximum equivalent plastic strain. Finally, the third frame applies for the analysis with the Tresca criteria of failure.

Each material failure criterion corresponds to a different strain energy density. Nevertheless, this fact did not significantly affect the total strain energy absorbed by the liftframe model nor the force vs displacement results, which are shown respectively in Figures 9 and 10. One can see that the analysis where the 12% maximum equivalent plastic strain criteria was applied the liftframe model split with 1.9 kJ of strain energy. In the analysis where the 18% maximum equivalent plastic strain criteria was applied, the total strain energy was 2.2 kJ at the instant of rupture. And in the third analysis, where the Tresca criteria was applied the liftframe model split with 1.85 kJ of strain energy. These results are summarised in Table 1 below.

Material Failure Criteria	Energy Absorbed at Rupture	Displacement at Rupture
12% max. eq. plast. strain	1.90 kJ	62 mm
18% max. eq. plast. strain	2.20 kJ	66 mm
Tresca	1.85 kJ	54 mm

Table 1 - Energy absorbed at rupture.

5. Comparison with Experimental Results

In 1984, a full-scale test on a Lynx airframe[15] was carried out, as part of an experimental program undertaken to investigate the behaviour of a conventional helicopter structure under dynamic crash conditions. The helicopter structure was fully instrumented and fitted with representative transmission and rotor weights. It was dropped vertically onto a rigid surface with an impact velocity of 8.2 m/s.

Comprehensive instrumentation provided deceleration and displacement data at specific locations on the test airframe. This and a complete film and photographic coverage, supplied valuable information on structural failure modes and energy absorption characteristics of various elements of the helicopter airframe. Though the specific force vs displacement curve for the helicopter liftframe was not obtained in this experiment, enough data about this structure behaviour could be used for the numerical simulation results evaluation.

Figure 11 shows a general view of the starboard half of the main liftframe after the drop test. It exhibited failures close to the cabin floor level, as occurred in the analysis discussed above. These failures initiated at the liftframe web-flange intersections and at the bottom horizontal stiffeners. In addition, the test confirmed that under the vertical impact condition, the liftframe would not be capable of absorbing the high masses kinetic energy and should really split.

There is particularly good agreement with the maximum load calculated in the analyses. According to the test report, the average value (for the port and the starboard sides) of the acceleration peak of the main gear box front feet was 88g. Those feet practically coincide with the liftframe loads application points. The dummy main-gear-box-main-rotor assembly used in the test weighted 885kg. Assigning 1/4 of this dynamic load to each foot of the main gear box, the peak can be estimated by:

$$P_{\max} = 1/4 \times 885 \times 88 \times 9.81 = 1.9 \times 10^5 \text{ N},$$

which is the same value observed in the 8m/s crash (see Figure 5).

Summarizing, it can be said that the numerical results show good agreement with the available test data.

6. Conclusions

MSC/DYTRAN was used to determine the collapse characteristics of the Lynx helicopter main liftframe, for the vertical crash case. The analysis was performed for crashworthiness assessment purposes and intended to simulate the vertical impact case with landing gears retracted as specified by current requirements. The mode of failure was characterized by the buckling of the lower part of the structure and of its vertical flanges. All the relevant plastic deformation was concentrated in these areas. In addition, the influence of the crushing velocity and the influence of the material failure criteria were investigated.

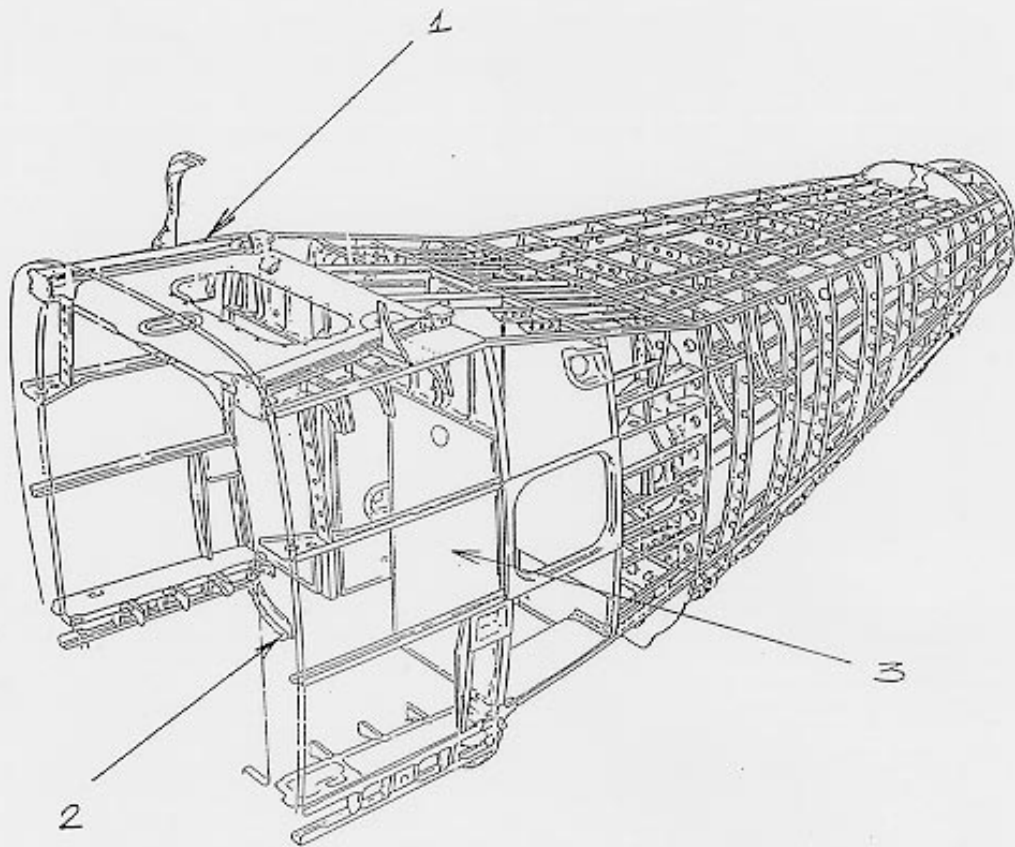
The main conclusions are:

- MSC/DYTRAN is a powerful tool for crashworthiness analysis.
- The crushing velocity affected the predicted mode of failure: at 4m/s it presented torsional buckling; and at 8m/s it was characterized by bending/axial failure;
- The material failure criteria did not significantly affect the collapse mechanism nor the force vs displacement results;

- The collapse characteristics needed for the hybrid analysis were defined and the model built herein can be used as part of a finite element model of the entire helicopter.

References

- [1]. Military Standard, MIL-STD-1290A (AV), Light Fixed and Rotary-Wing Aircraft Resistance, Department of Defense, Washington, DC, Sep 1988.
- [2]. Saczalski, K.J. and Pilkey, W.D. - Techniques for Predicting Vehicles Crash Impact Response. In *Aircraft Crashworthiness* (Edited by K. Saczalski, G.T. Singley III, W.D. Pilkey and R.L. Huston), pp. 467-484. University Press of Virginia, Charlottesville, VA, 1975.
- [3]. Alfaro-Bou, E. and al. - Simulation of Aircraft Crash and Its Validation. In *Aircraft Crashworthiness* (Edited by K. Saczalski, G.T. Singley III, W.D. Pilkey and R.L. Huston), pp. 485-498. University Press of Virginia, Charlottesville, VA, 1975.
- [4]. Pifko, A.B. and Winter, R. - Theory and Application of Finite Element Analysis to Structural Crash Simulation. *Computers & Structures*, vol. 13, pp. 277-285, 1981.
- [5]. Belytschko, T. - On Computational Methods for Crashworthiness. *Computers & Structures*, vol. 42, pp. 271-279, 1992.
- [6]. Wittlin, G. and Gamon, M.A. - Experimental Program for the Development of Improved Helicopter Structural Crashworthiness Analytical and Design Techniques. USAAMRDL Technical Report 72-72, May 1973.
- [7]. Hallquist, J.O. - Theoretical Manual for DYNA3D. Report UCID-19041, Lawrence Livermore National Laboratory, Livermore, CA, 1983.
- [8]. Cook, R. D., Malkus, D. S., and Plesha, M. E. - *Concepts and Applications of Finite Element Analysis*. John Wiley & Sons, 3rd ed. New York, 1989.
- [9]. Military Handbook MIL-HDBK-5(F) - Metallic Materials and Elements for Aerospace Vehicle Structures, Department of Defense, Washington, DC, 1990.
- [10]. Zukas, J.A. & al - *Impact Dynamics*. John Wiley & Sons, New York, 1982.
- [11]. Levine, H.S. & al - Crash Analysis of a C-141B Transport Using an Explicit Nonlinear Finite Element Code. *Proceedings of The 2nd International KRASH User's Seminar*, Cranfield Impact Centre Ltd, Cranfield, England, Jun 1995.
- [12]. Stronge, W.J. and Yu, T.X. - *Dynamic Models for Structural Plasticity*. Springer-Verlag, London, 1993.
- [13]. Duffey, T.A. Dynamic Rupture of Shells. In *Structural Failure*. By Wierzbicki, T. and Jones, N., John Wiley & Sons, New York, 1989.
- [14]. Kenefeck, M. - Drop Test on a Lynx Helicopter. In *Structural Impact and Crashworthiness*, vol 2 Edited by Morton, J.), pp. 733-744, London, 1984.



- 1- Main gear box support beam
- 2 - Main liftframe
- 3 - Bulkhead

Fig. 1 - Lynx rear fuselage structure.

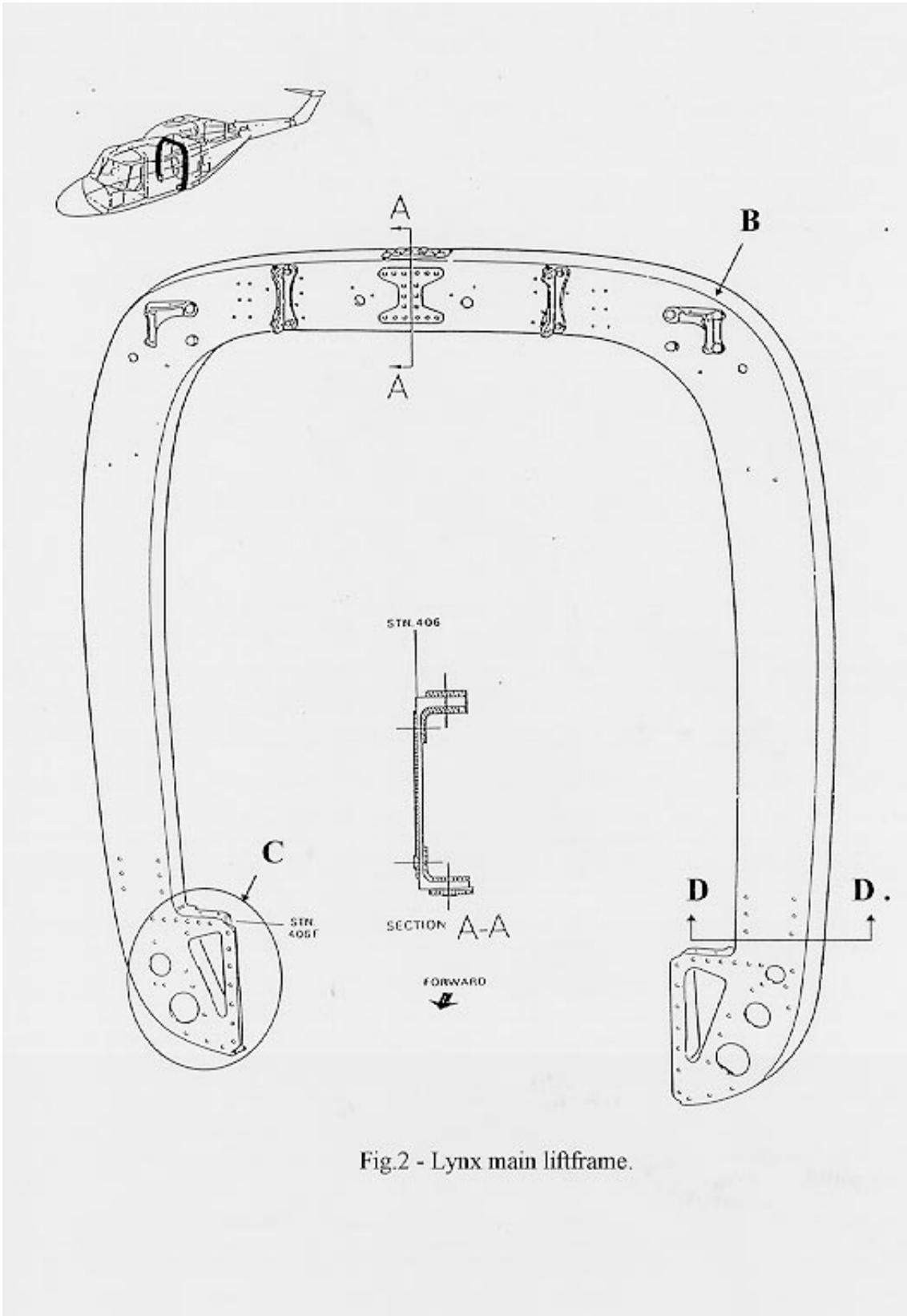


Fig.2 - Lynx main liftframe.

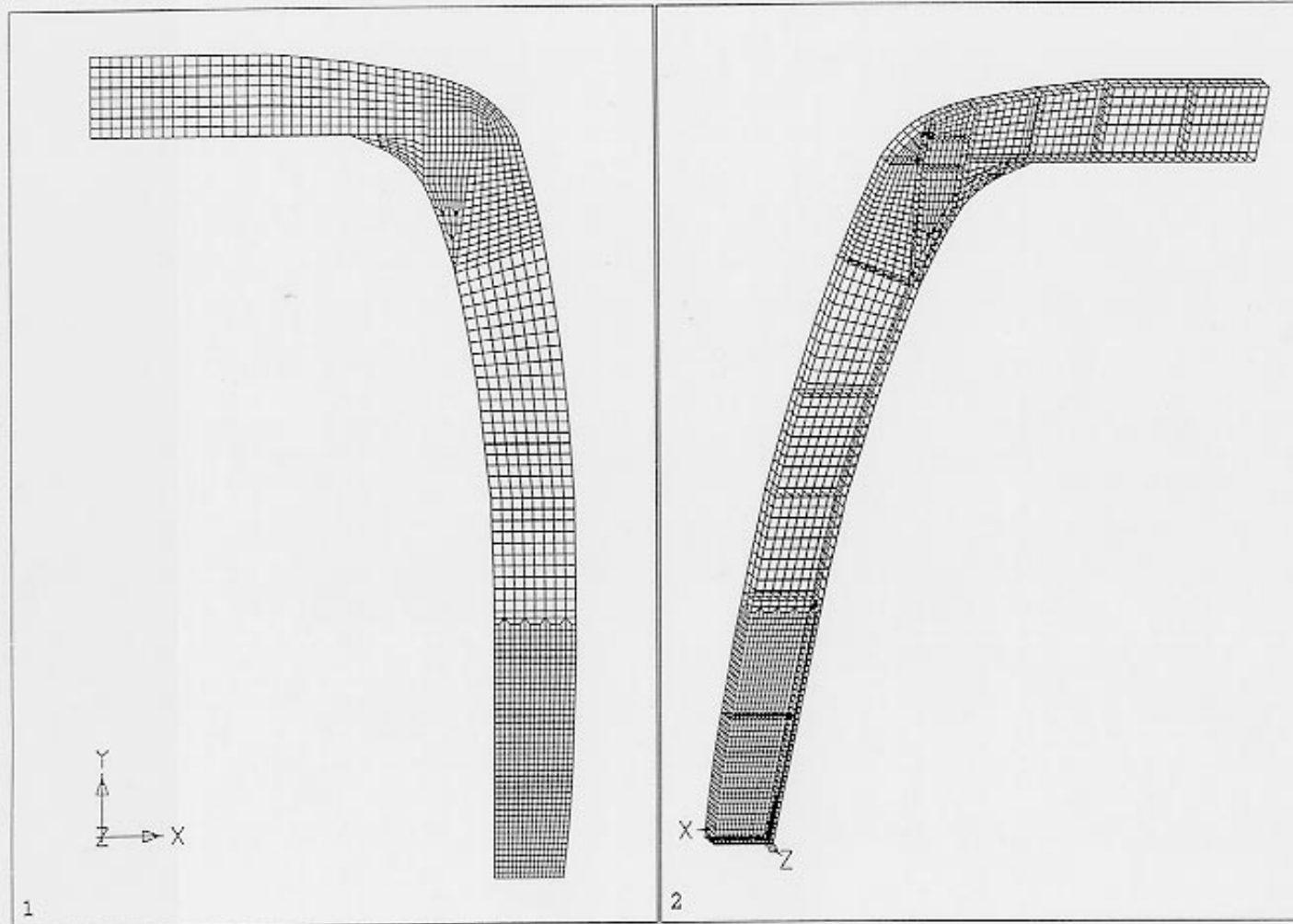
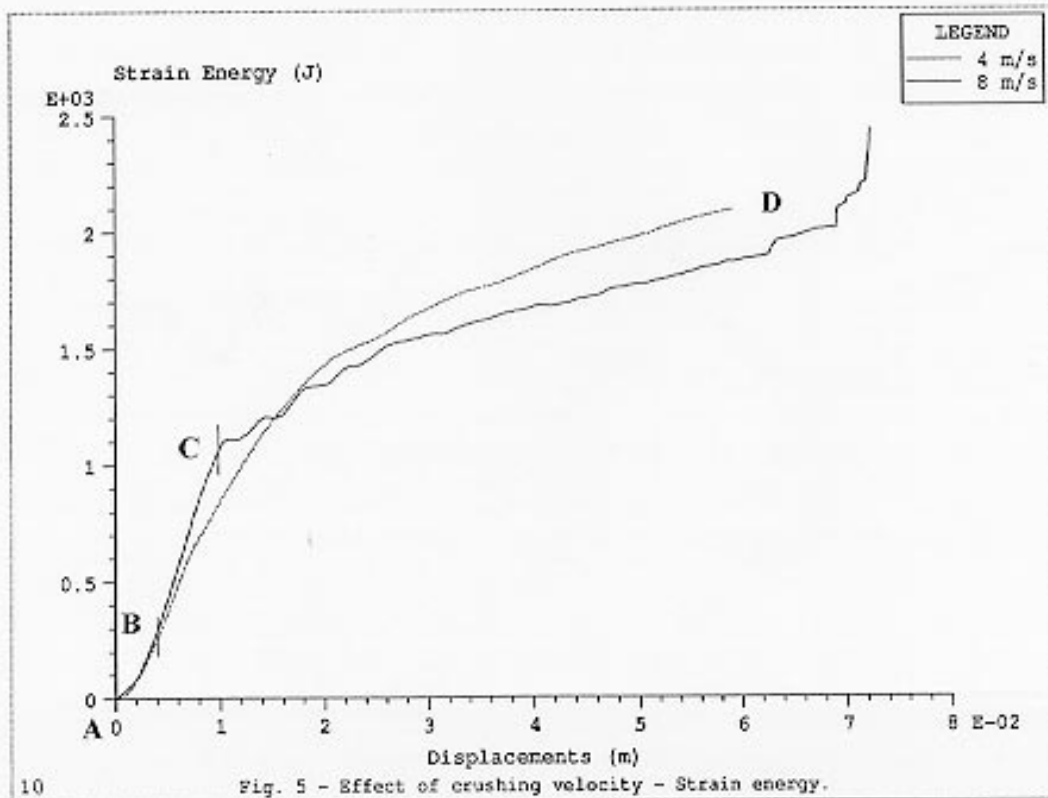
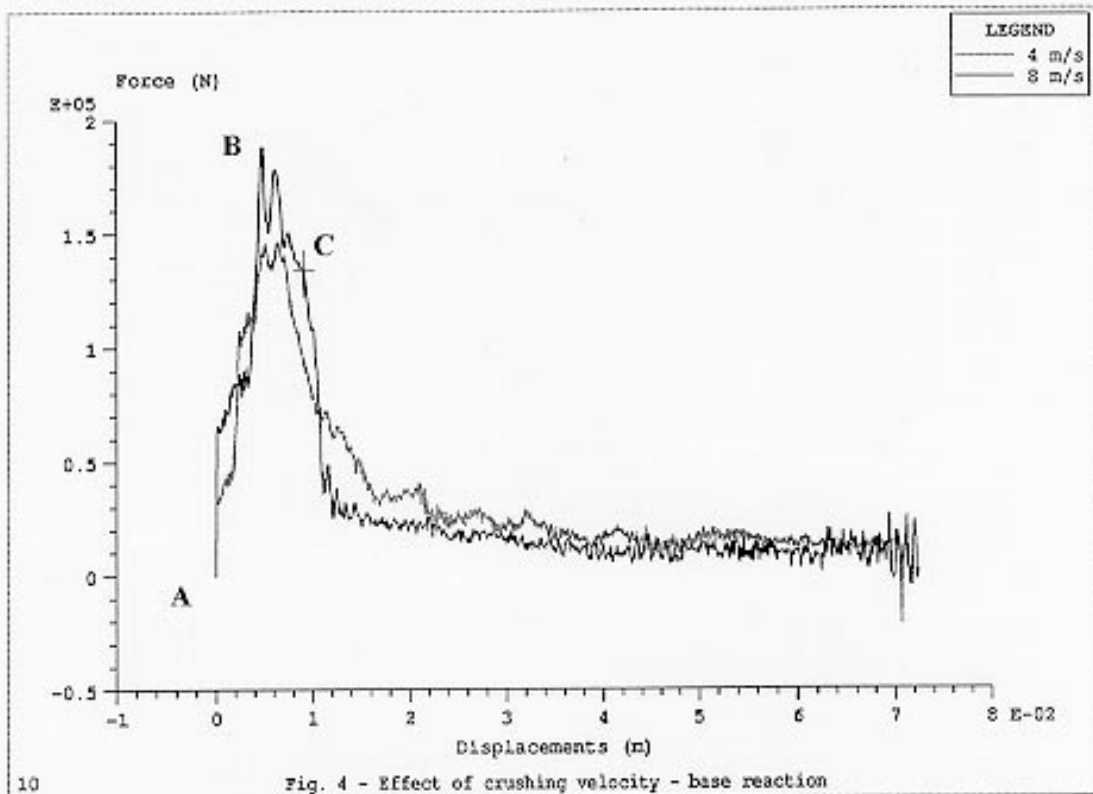


Fig 3 - Lynx helicopter port side half main liftframe model.



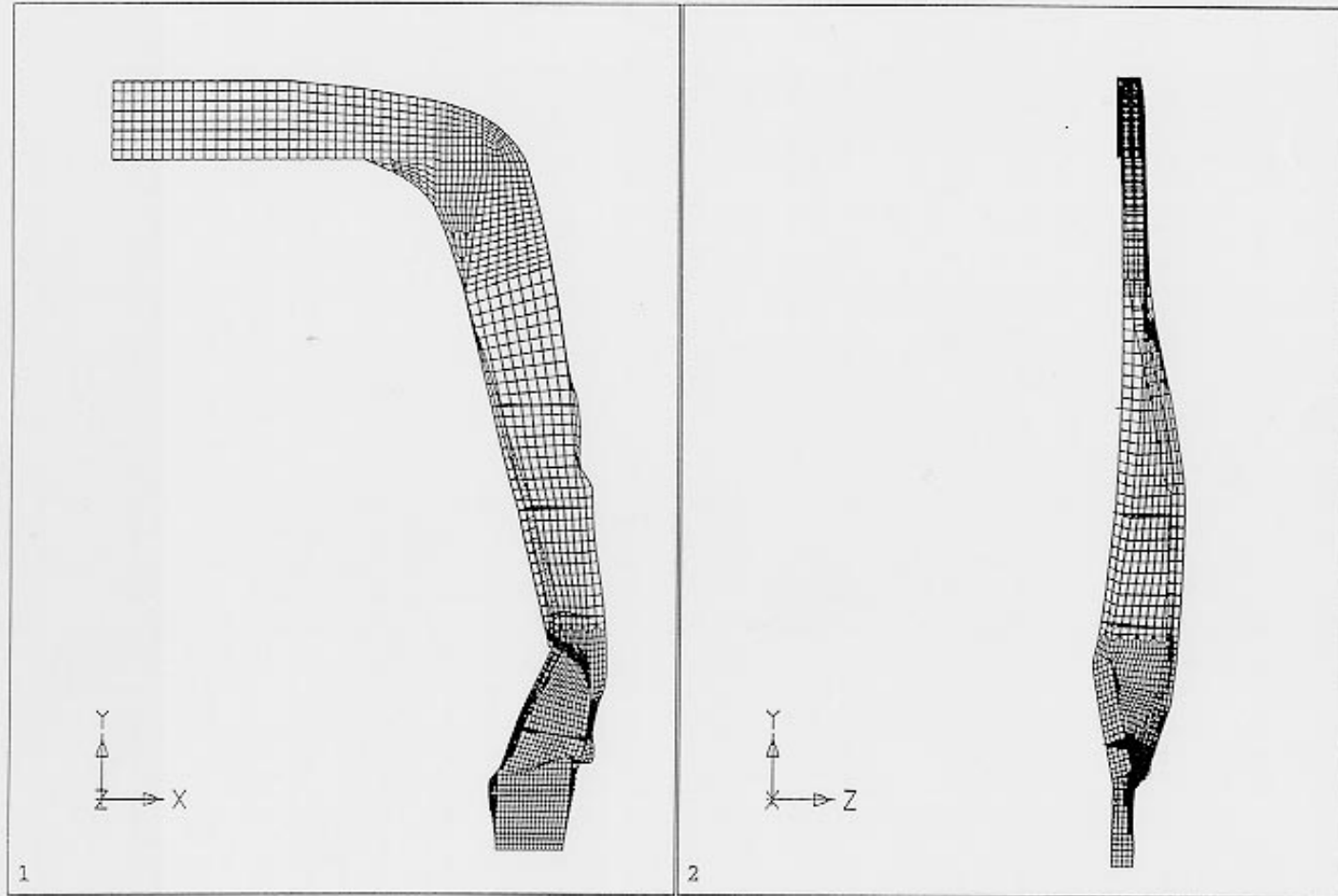


Fig. 6 - Model crashed at 4m/s - 60 mm of displacement.

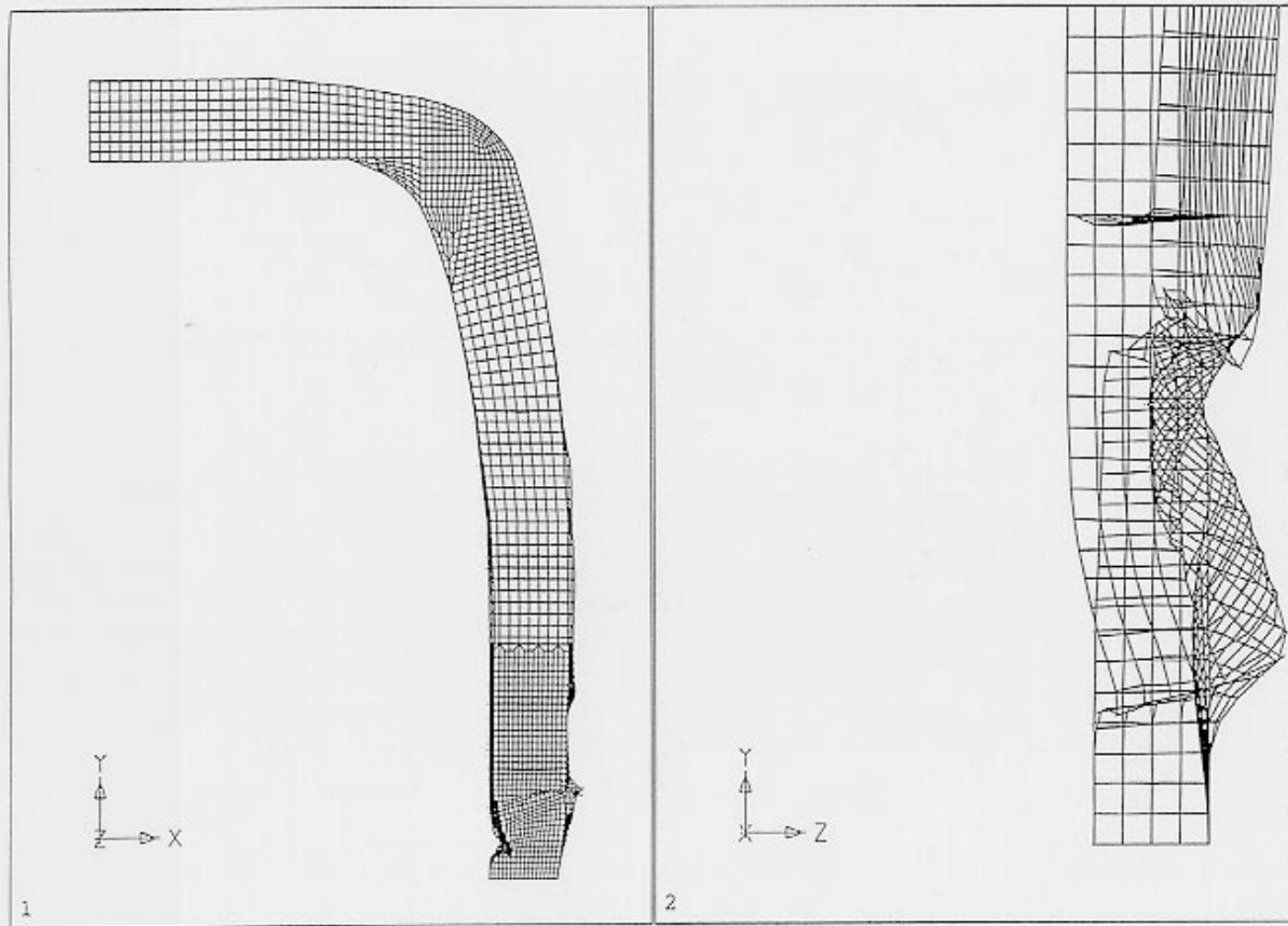


Fig.7 - Model crashed at 8m/s - 40 mm of displacement.

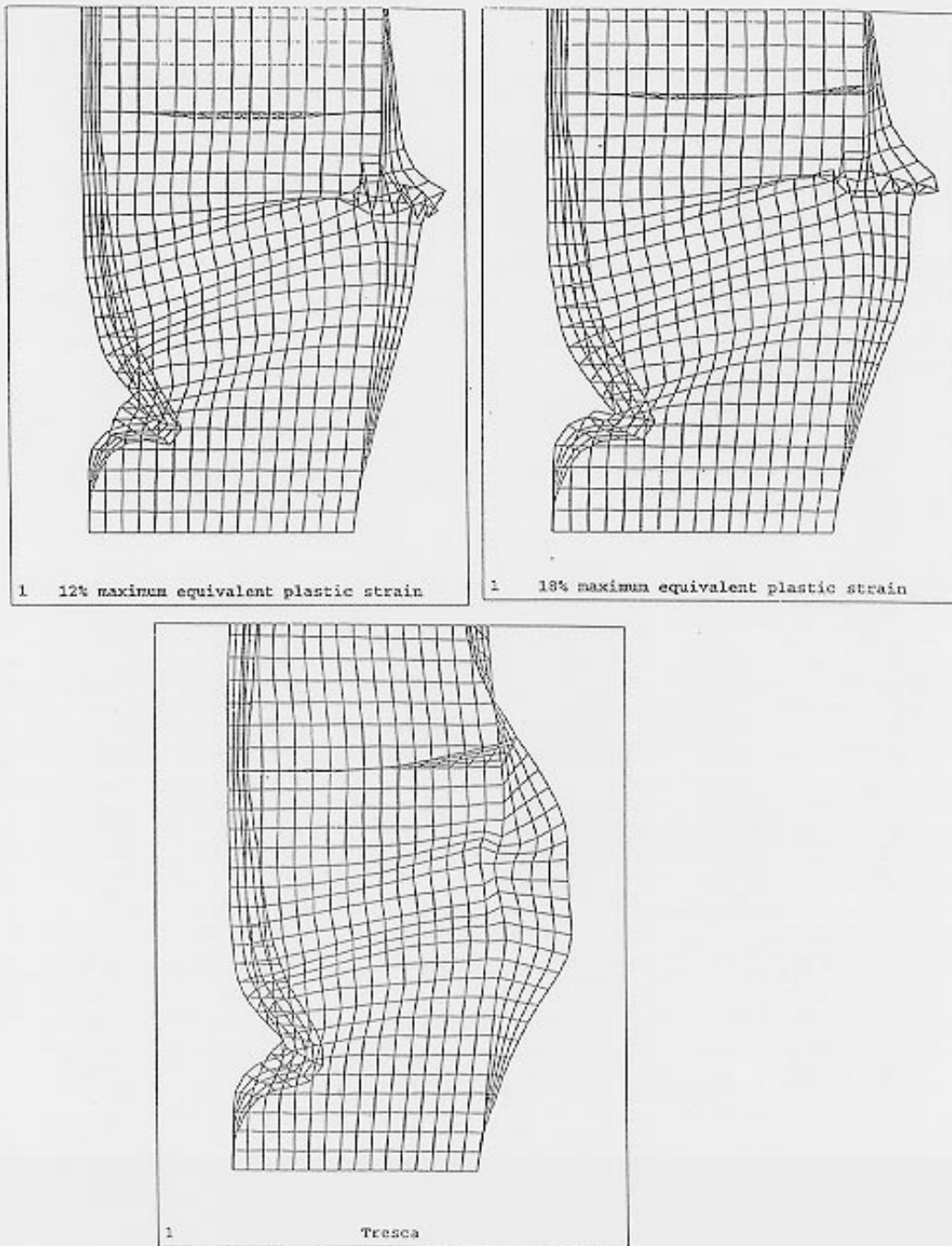


Fig. 8 - Modes of failure for three different material failure criteria.

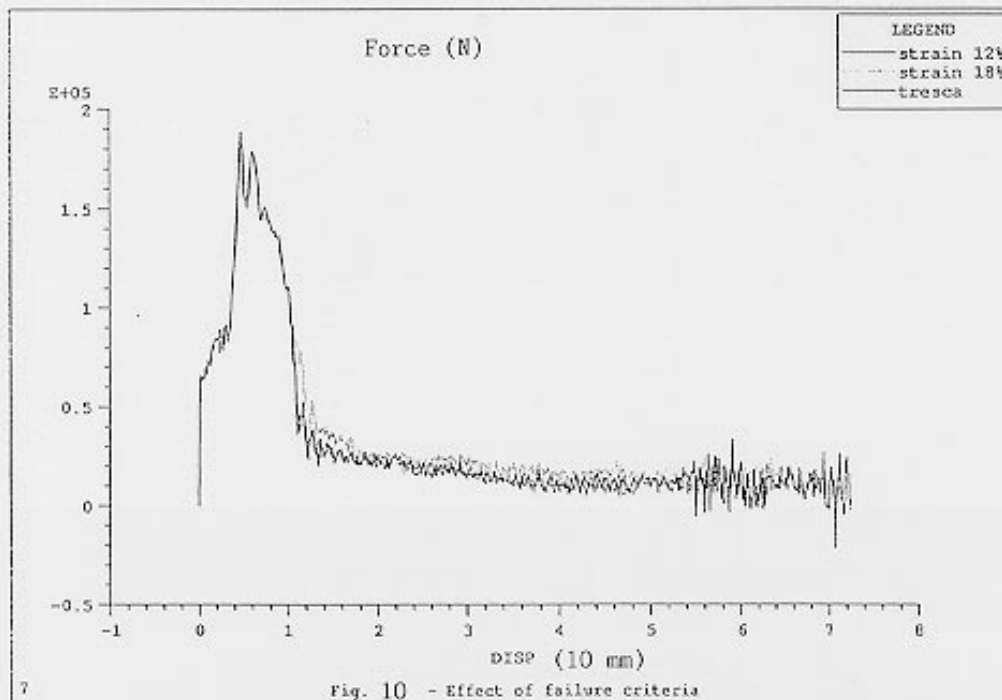
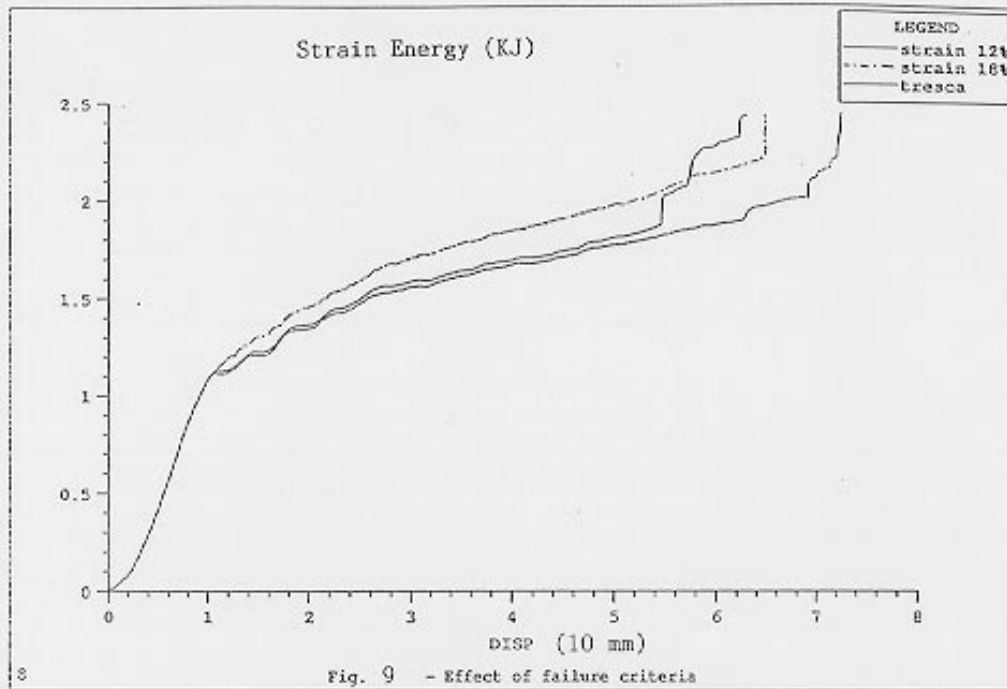




Fig. 11 - Vertical drop test- Failure of starboard main liftframe.